

Calculation of Plane-of-Symmetry Boundary Layers with a Modified k - ϵ Model

C. H. Sohn,* D. H. Choi,[†] and M. K. Chung[‡]

Korea Advanced Institute of Science and Technology, Seoul, Korea

The effects of vortex stretching and normal stresses on the development of turbulent boundary layers are numerically investigated by adopting both the vortex stretching invariant and the preferential normal stress concept in the dissipation equation of the standard k - ϵ model. An application of the proposed ϵ equation to a plane-of-symmetry boundary-layer flow reveals that the preferential normal stress terms under the flow convergence reduces the turbulent kinetic energy k and the eddy viscosity ν_t , whereas the squeezing of vorticity augments them, consistent with experimental observation. Comparison of predicted profiles of various flow variables by the proposed model with those by other k - ϵ and mixing length models demonstrates that the present ϵ equation improves markedly the computational accuracy of the relatively complex flow in a plane of symmetry.

I. Introduction

THE flow along a plane of symmetry is of considerable practical interests in the study of the flow over three-dimensional bodies such as ship hulls, aircraft fuselages, missiles, and automobiles. Numerical solution of the flow in a plane of symmetry can be used to provide the boundary conditions for the calculation of the boundary layer on the body and it can also be used to check the solution over an entire body. The solution of the boundary-layer equations in the plane of symmetry is relatively easy to obtain. Nevertheless, since the boundary layer is subjected to flow convergence and divergence depending on the relative flow direction over the surface, it provides a good opportunity to study such effect on the development of the boundary-layer flow.

Recently, detailed turbulence measurements were made in the plane of symmetry of a body of revolution by Patel and Baek.¹ They demonstrated the direct effect of the flow divergence and convergence on the turbulence structure: flow convergence reduces the length scale and the eddy-viscosity and, therefore, the Reynolds stresses and, on the other hand, the flow divergence augments them. These measurements provide turbulence data as well as the mean velocity field against which turbulence models can be verified.

They also performed a calculation of the turbulent boundary layer in a plane of symmetry utilizing the mixing length model of Cebeci and Smith² and showed that such a model cannot properly take account of the length scale variation depending on the flow convergence or divergence.³ Since the turbulence length scale is closely related to the rate of kinetic energy dissipation ϵ , when the popular k - ϵ model is applied to the plane-of-symmetry flows, the ϵ equation must contain a model term (or terms) that represents the effect of flow convergence or divergence.

Pope⁴ introduced a term that is interpreted as additional generation of dissipation rate ϵ of turbulent kinetic energy due to the stretching of turbulent vortex tube by the mean flow. The term is zero in a plane two-dimensional flow since the

mean vortex lines do not change their length. On the other hand, for a plane-of-symmetry flow, they are stretched or squeezed as the flow diverges or converges, respectively, and, thus, the additional term directly influences ϵ and consequently the Reynolds stresses. Meanwhile, Hanjalic and Launder⁵ pointed out the energy transfer rate across the spectrum is preferentially promoted by irrotational deformations (or Reynolds normal stresses), and they showed that a modification of ϵ equation due to such preferential normal stresses gives improved results for decelerated flows. Rodi and Scheuerer⁶ also found that this modified k - ϵ model yields good predictions for two-dimensional flows with a strong adverse pressure gradient. In view of the fact that the plane-of-symmetry flows exhibit both the stretching or squeezing of the turbulent vortex tube and the nonzero irrotational deformation, it is believed that both proposed models of Pope⁴ and Hanjalic & Launder⁵ must be combined to predict such flows. The present paper presents a new ϵ equation that includes both mechanisms and compares its prediction performance with those of various other existing models for the plane-of-symmetry flows.

II. Governing Equations

Consider a boundary layer developed along a plane of symmetry on a body of revolution. Because of the symmetry, the circumferential velocity component becomes zero and the derivatives of all of the dependent variables in the circumferential direction vanish except that of the circumferential velocity component. This, in effect, decouples the plane-of-symmetry equations from the equations governing the flow elsewhere over the body.

Following Nash and Patel,⁷ the boundary-layer equations for an incompressible flow in a body-fitted coordinate system defined in Fig. 1 are

$$\frac{1}{h_1} \frac{\partial U}{\partial x} + \frac{\partial V}{\partial y} + W_1 + K_{31}U = 0 \quad (1)$$

$$\frac{U}{h_1} \frac{\partial U}{\partial x} + V \frac{\partial U}{\partial y} + \frac{1}{h_1} \frac{\partial}{\partial x} \left(\frac{p}{\rho} \right) + \frac{\partial}{\partial y} (\overline{uv}) - \nu \frac{\partial^2 U}{\partial y^2} = 0 \quad (2)$$

$$\begin{aligned} \frac{U}{h_1} \frac{\partial W_1}{\partial x} + V \frac{\partial W_1}{\partial y} + W_1^2 + 2K_{31}UW_1 + \frac{1}{h_3^2} \frac{\partial^2}{\partial z^2} \left(\frac{p}{\rho} \right) \\ + \frac{\partial W_2}{\partial y} - \nu \frac{\partial^2 W_1}{\partial y^2} = 0 \end{aligned} \quad (3)$$

Received Jan. 23, 1990; revision received March 12, 1990. Copyright © 1990 by the American Institute of Aeronautics and Astronautics, Inc. All rights reserved.

*Graduate Student, Department of Mechanical Engineering. Member AIAA.

[†]Professor, Department of Mechanical Engineering. Member AIAA.

[‡]Professor, Department of Mechanical Engineering.

where

$$W_1 = \frac{1}{h_3} \frac{\partial W}{\partial z}, \quad W_2 = \frac{1}{h_3} \frac{\partial}{\partial z} (\overline{vw})$$

Here, (U, V, W) represent the mean velocity components in the (x, y, z) directions, respectively, $-\overline{uv}$ and $-\overline{vw}$ the Reynolds shear stresses, p the pressure, ρ the density, ν the kinematic viscosity, and h_1 and h_3 the metric coefficients in the x and z directions.

Although the crossflow velocity W , in the circumferential direction is locally zero, its circumferential gradient W_1 is nonzero and is a measure of the lateral convergence or divergence of streamlines into, or out of, the plane of symmetry. Equation (3) is obtained by differentiating the z -momentum equation with respect to z and evaluating all terms at $z = 0$.

If the shape of the body is prescribed by $r(X)$, where the coordinate X is the distance measured along the axis of the body from the nose, the metric coefficients and the curvature parameter K_{31} are given as

$$h_1 = \left[1 + \left(\frac{\partial r}{\partial X} \right)^2 \right]^{1/2}, \quad h_3 = r(X), \quad K_{31} = \frac{1}{h_1 h_3} \frac{\partial h_3}{\partial X} \quad (4)$$

The boundary conditions are

$$U = W_1 = 0 \quad \text{at } y = 0 \quad (5a)$$

$$U = U_e, \quad W_1 = W_{1e} \quad \text{as } y \rightarrow \delta \quad (5b)$$

where the subscript e denotes the edge condition. Finally, the Bernoulli equation gives the following relationships for the pressure gradients, which need to be prescribed for the calculation:

$$-\frac{1}{h_1} \frac{\partial}{\partial x} \left(\frac{p}{\rho} \right) = \frac{U_e}{h_1} \frac{\partial U_e}{\partial x} \quad (6a)$$

$$-\frac{1}{h_3} \frac{\partial^2}{\partial z^2} \left(\frac{p}{\rho} \right) = \frac{U_e}{h_1} \frac{\partial W_{1e}}{\partial x} + W_{1e}^2 + 2K_{31} U_e W_{1e} \quad (6b)$$

III. Turbulence Model

A. Hanjalic and Launder's k - ϵ Model⁵ with Preferential Normal Stresses

Two variations of the standard k - ϵ model are examined in this study with the eddy viscosity hypothesis in the following form:

$$-\overline{uv} = \nu_t \frac{\partial U}{\partial y}, \quad -\overline{vw} = \nu_t \frac{\partial W}{\partial y}; \quad \nu_t = c_\mu \frac{k^2}{\epsilon} \quad (7)$$

where ν_t is a scalar eddy viscosity, k the turbulent kinetic energy, and ϵ the rate of dissipation. The distributions of k and ϵ are determined from the transport equations as follows:

$$\frac{U}{h_1} \frac{\partial k}{\partial x} + V \frac{\partial k}{\partial y} = \frac{\partial}{\partial y} \left[\left(\nu + \frac{\nu_t}{\sigma_k} \right) \frac{\partial k}{\partial y} \right] + P_k - \epsilon \quad (8)$$

$$\frac{U}{h_1} \frac{\partial \epsilon}{\partial x} + V \frac{\partial \epsilon}{\partial y} = \frac{\partial}{\partial y} \left[\left(\nu + \frac{\nu_t}{\sigma_\epsilon} \right) \frac{\partial \epsilon}{\partial y} \right] + c_{\epsilon 1} \frac{\epsilon}{k} P_k - c_{\epsilon 2} \frac{\epsilon^2}{k} \quad (9)$$

where

$$P_k = P_{k,s} + P_{k,n} = -\overline{uv} \frac{\partial U}{\partial y} - (\overline{u^2} - \overline{v^2}) \frac{1}{h_1} \frac{\partial U}{\partial x} + (\overline{v^2} - \overline{w^2}) (W_1 + K_{31} U) \quad (10)$$

denotes the generation of turbulent kinetic energy and c_μ , σ_k , σ_ϵ , $c_{\epsilon 1}$, and $c_{\epsilon 2}$ are model constants whose values are 0.09, 1.0, 1.3, 1.44, and 1.92, respectively. $P_{k,n}$ represents the underlined terms in Eq. (10), which involve normal stresses. Since the k - ϵ model does not provide values of $\overline{u^2}$, $\overline{v^2}$, and $\overline{w^2}$ explicitly, Hanjalic and Launder⁵ used the experimental values of these quantities related to the turbulent kinetic energy. This approach is also adopted in the present study, and the values of $\overline{u^2}$, $\overline{v^2}$, and $\overline{w^2}$ are approximated by $\overline{u^2}/k = 1.05$, $\overline{v^2}/k = 0.40$, and $\overline{w^2}/k = 0.55$ according to Patel and Baek.¹

Hanjalic and Launder⁵ pointed out that normal stresses are more effective than shear stresses in promoting the transfer of turbulent kinetic energy from larger eddies to smaller ones. They reflected such preferential transfer mechanism into the ϵ equation by multiplying the term $P_{k,n}$ by a constant $c_{\epsilon 3}$, which is larger than $c_{\epsilon 1}$ for the shear stress part $P_{k,s}$ and, thus, P_k in Eq. (9) is replaced by a modified form P_ϵ as follows:

$$P_\epsilon = P_{k,s} + \frac{c_{\epsilon 3}}{c_{\epsilon 1}} P_{k,n} \quad (11)$$

Here, the empirical constant $c_{\epsilon 3}$ was given a value of 4.44, and they found that the spreading rate of the round jet is predicted better than that by the standard k - ϵ model. Rodi and Scheuerer⁶ tested the Hanjalic and Launder model and they also obtained good predictions for moderately and strongly decelerated flows. For the convergent flows ($W_1 < 0$), the second term in $P_{k,n}$ becomes positive since $\overline{v^2} < \overline{w^2}$ in most regions, which results in increase of ϵ and, thus, decrease of ν_t . This effect is consistent with the experimental observation of Patel and Baek.¹

Retaining the normal stress terms in the equation may seem somewhat incompatible with the thin boundary-layer approximation as these terms, normally, are of higher order. However, as we shall see later, the terms play an important role in the relaxing adverse-pressure-gradient boundary layer and, therefore, are kept in the calculation. This view was also expressed by Cutler and Johnston⁸ in their recent experimental study of a relaxing turbulent boundary layer.

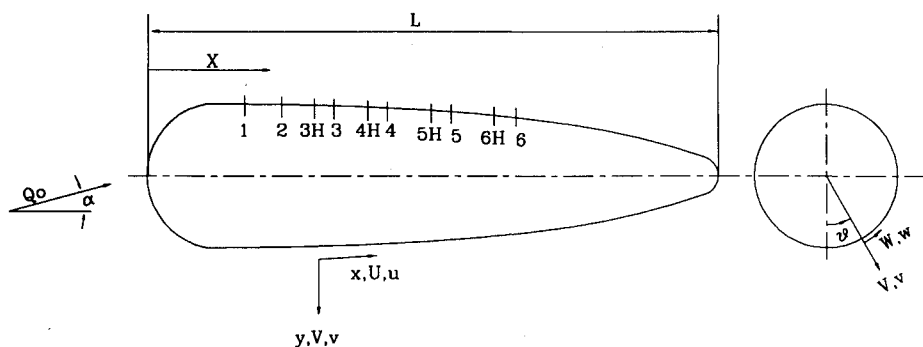


Fig. 1 Geometry of a combination body and coordinate system.

B. Inclusion of Pope's Modification for Vortex Stretching in the k - ϵ Model

The modification dealt with in this subsection was originally proposed by Pope⁴ for the round jet. There, he defined the nondimensional measure of vortex stretching by the invariant $\chi = \omega_{ij}\omega_{jkski}$, where

$$s_{ij} = \frac{1}{2} \frac{k}{\epsilon} \left(\frac{\partial U_i}{\partial x_j} + \frac{\partial U_j}{\partial x_i} \right), \quad \omega_{ij} = \frac{1}{2} \frac{k}{\epsilon} \left(\frac{\partial U_i}{\partial x_j} - \frac{\partial U_j}{\partial x_i} \right) \quad (12)$$

In a plane of symmetry, the invariant χ becomes

$$\chi = \frac{1}{4} \left(\frac{k}{\epsilon} \right)^3 \left(\frac{\partial U}{\partial y} - \frac{1}{h_1} \frac{\partial V}{\partial x} \right)^2 (W_1 + K_{31}U) \quad (13)$$

It can be seen from Fig. 2 that there is a distinct relationship between the vortex stretching and the flow convergence or divergence for a plane-of-symmetry flow. The stretching term χ is zero in two-dimensional flows ($W_1 = 0$ and $K_{31} = 0$) so that the modification has no effect. For axisymmetric flow ($W_1 = 0$), the vortex is stretched as the radius of the body shape $r(X)$ increases ($K_{31} > 0$) or it is squeezed as the radius decreases ($K_{31} < 0$). In a plane of symmetry, the vortex is stretched by the divergent flow ($W_1 > 0$) and squeezed by the convergent flow ($W_1 < 0$). As the vortex is stretched by the positive strain s_{ij} , it increases in frequency and decreases in width to conserve the angular momentum, therefore, leading to greater dissipation ϵ and, consequently, eddy viscosity ν_t is reduced. The influence of squeezing is opposite to that of stretching.

Then, if these effects of the vortex stretching or squeezing are taken into account, the dissipation rate equation is modified to have the final form as

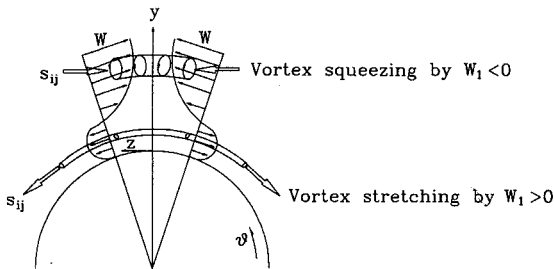


Fig. 2 Illustration of flow convergence and divergence flow on the plane of symmetry.

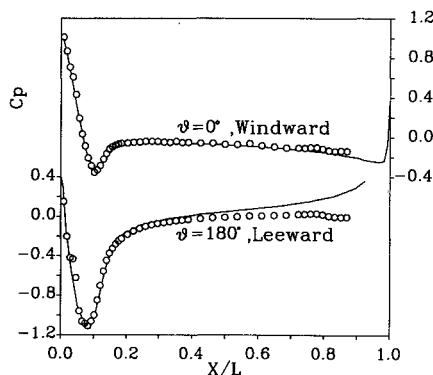


Fig. 3 Surface pressure distribution in the planes-of-symmetry of the combination body, $\alpha = 15$ deg: \circ experiment; — potential flow theory.

$$\frac{U}{h_1} \frac{\partial \epsilon}{\partial x} + V \frac{\partial \epsilon}{\partial y} = \frac{\partial}{\partial y} \left[\left(\nu + \frac{\nu_t}{\sigma_\epsilon} \right) \frac{\partial \epsilon}{\partial y} \right] + c_{e1} \frac{\epsilon}{k} P_\epsilon - \frac{\epsilon^2}{k} (c_{e2} - c_{e4} \chi) \quad (14)$$

The empirical constant c_{e4} was given a value 0.79 by Pope⁴ to reproduce the growth rate of the round jet. The value was chosen without Hanjalic and Launder's preferential normal stress term in Eq. (14). With this term included, however, we found that $c_{e4} = 0.4$ yields correct spreading rate of the round jet. Note that for two-dimensional flows, the modified equation becomes the same as that given by Hanjalic and Launder's since there is no vortex stretching.

IV. Computational Results and Discussion

To assess the performance of the present model consisting of Eqs. (8), (10), and (14), the plane-of-symmetry flow measured by Patel and Baek¹ is selected as a test flow. They measured mean velocities and turbulent fluctuations in the planes of symmetry of a body of revolution, which is a combination of a hemispheric nose and a half-spheroid (see Fig. 1), at 15 deg incidence and a Reynolds number of 1.86×10^6 . The mean velocity data were obtained at six locations, $X/L = 0.169, 0.234, 0.326, 0.419, 0.530$, and 0.641 labeled as stations 1–6, but the turbulence data were measured at four locations, $X/L = 0.291, 0.384, 0.495$, and 0.606 , which are labeled as stations 3H–6H.

The numerical scheme used in the present study is the Crank-Nicolson method of Chang and Patel,⁹ and the experimental distributions of U_e and W_{1e} are prescribed as boundary conditions.

In order to avoid the uncertainty of transition, the calculation is started at $X/L = 0.169$, which is the most upstream station of the measurement. The initial profile for U is given by the experiment, whereas that for W_1 is adopted from the profile used in Patel and Baek.³ The profiles of k and ϵ at this location are specified by means of the following relationships⁶:

$$k = \bar{u}\bar{v}/0.3 \quad (15a)$$

$$\epsilon = \frac{k^{3/2}}{L} \left(1 + \frac{c_\epsilon}{k^{1/2} L / \nu} \right) \quad (15b)$$

where $-\bar{u}\bar{v}$ is provided from the eddy-viscosity relation of Cebeci and Smith.² Here, the length scale L is estimated by $L = C_D \min \{ \kappa y, \lambda \delta \}$ and the empirical constants are $C_D = 6.41$, $c_\epsilon = 13.2$, $\lambda = 0.085$, and $\kappa = 0.41$.

Besides the present turbulence model, calculations have been performed with other existing models: the zero-equation model of Cebeci and Smith² (denoted by CS), the standard k - ϵ

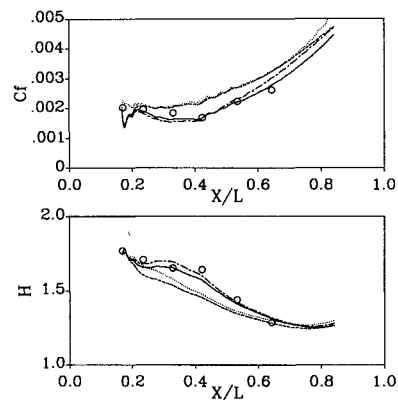


Fig. 4 Comparison of predictions of skin friction coefficient and shape factor with experimental results on the leeward plane of the combination body, $\alpha = 15$ deg and $Re = 1.86 \times 10^6$: \circ experiment; — present model; ---- ST models; CS model; -.-.- HL model.

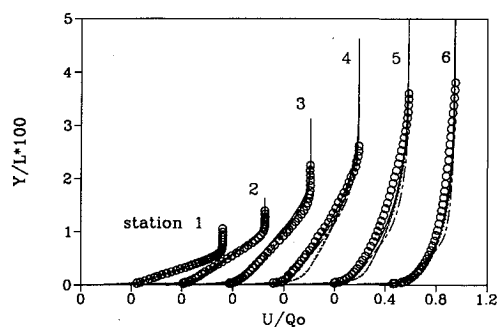


Fig. 5 U -velocity profiles on the leeward plane of the combination body, $\alpha = 15$ deg and $Re = 1.86 \times 10^6$: \circ , experiment; —, present model; ----, ST model; CS model; - · - · - HL model.

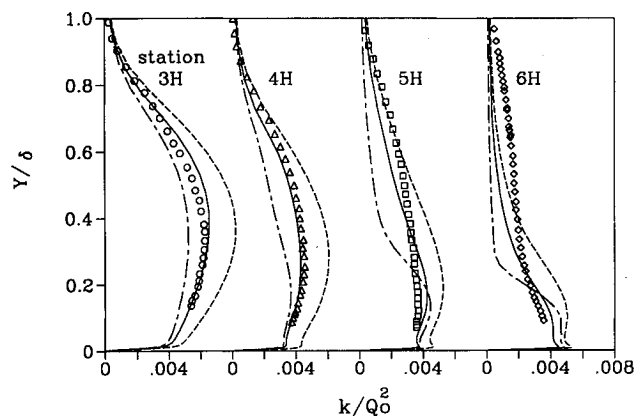


Fig. 6 Turbulent kinetic energy profiles on the leeward plane of the combination body, $\alpha = 15$ deg and $Re = 1.86 \times 10^6$: \circ , Δ , \square , \diamond experiment; —, present model; ----, ST model; - · - · - HL model.

model (ST), and the modified k - ϵ model of Hanjalic and Launder (HL). It should be pointed out here that, in order to treat the low Reynolds number effect near the wall, the two-layer approach of Chen and Patel^{10,11} has been incorporated in all two-equation models. Therefore, the model designated as ST is actually the two-layer model of Chen and Patel. However, since the other models also use the same approach, the models are designated CS, ST, and HL to distinguish one from another.

The boundary-layer behavior is more complex on the leeward side ($\theta = 180$ deg) of a body at incidence than the windward side ($\theta = 0$ deg) since the stronger adverse pressure gradient in the initial region (see Fig. 3) as well as the flow convergence ($W_1 < 0$) into the plane of symmetry cause the boundary layer to grow rapidly and to generate the streamwise vortex embedded inside the thickening boundary layer. The thickening of the boundary layer is large and accompanies a substantial viscous-inviscid interaction.¹² The computational results for the leeward plane of symmetry are compared with the experiments in Figs. 4–8.

Figure 4 shows the skin friction coefficients C_f and shape factors H . The initial deviation in C_f suggests that the initial values of k and ϵ are not correct. However, no attempt has been made to correct the discrepancy as it recovers the proper value in a few steps. It is seen that the CS and ST models generally overpredict the skin friction and underestimate the shape factor H . Although, the HL model correctly simulates the influence of the initial strong adverse pressure gradient on C_f , this too yields higher values of C_f for $X/L > 0.5$. It is evident from the figure that the results with the present model compare most favorably with the data. The reason for this may be given as follows. The boundary layer along the lee-

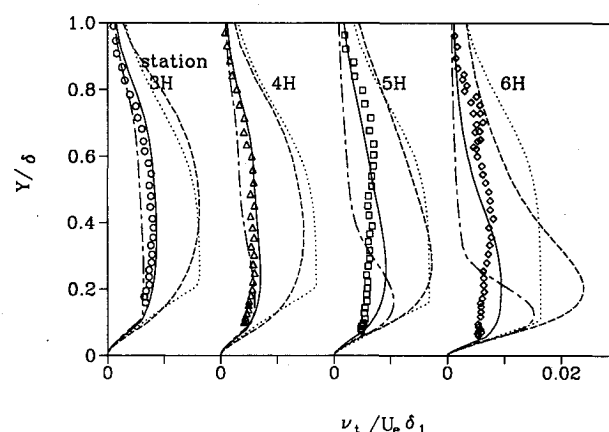


Fig. 7 Eddy-viscosity profiles on the leeward plane of the combination body, $\alpha = 15$ deg and $Re = 1.86 \times 10^6$: \circ , Δ , \square , \diamond experiment; —, present model; ----, ST model; CS model; - · - · - HL model.

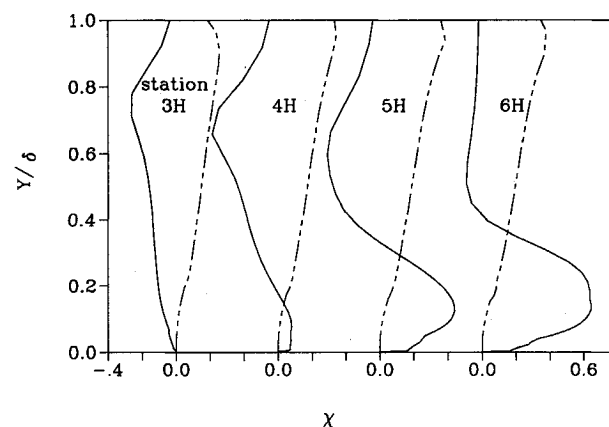


Fig. 8 Variation of vortex stretching parameter χ in the plane of symmetry boundary layer: —, leeward side; ----, windward side.

ward plane of symmetry, which is initially convergent, becomes divergent near the surface at $X/L \approx 0.3$. This region of divergence increases with downstream distance, resulting in a decrease in the eddy viscosity. Although the HL model performs better than the CS and ST models, it becomes less successful in the divergent region as it lacks the mechanism to take account of the stretching (or squeezing) effect. We will return to this point later in this section.

The velocity profiles are compared in Fig. 5. The CS and ST models overpredict the velocity in the near-wall region at stations 4 and 5, whereas the HL model predicts much thinner boundary layers at stations 5 and 6. The results with the present model, on the other hand, show good agreement with the data for the entire flowfield.

The behavior may be better illustrated in the turbulent kinetic energy and eddy viscosity distributions, which are in line with the prediction of the velocity profiles. The kinetic energy plotted in Fig. 6 is generally overpredicted by the ST model and underpredicted by the HL model. The latter predicts virtually zero turbulent kinetic energy in the outer part of the boundary layer at station 6H and, thus, makes the boundary layer thinner. Also, the underprediction noted at stations 3H and 4H, where the effect of the adverse pressure gradient and the flow convergence are expected to be strong, implies that the empirical constant $c_{\epsilon 3} = 4.44$ in the HL model may be too large. The result for the eddy viscosity is similar to that for the kinetic energy, as shown in Fig. 7. A significant departure, however, may be observed in the prediction of the ST and HL models in the near-wall region at stations 5H and

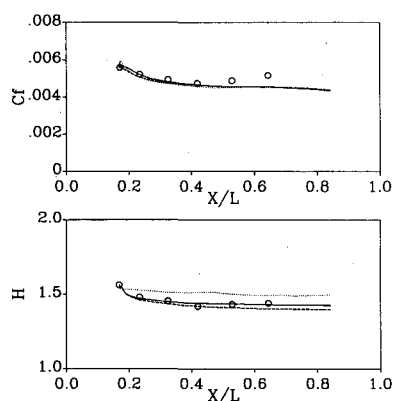


Fig. 9 Comparison of predictions of skin friction coefficient and shape factor with the experimental results on the windward plane of the combination body, $\alpha = 15$ deg and $Re = 1.86 \times 10^6$: o, experiment; -- present model; - - - ST model; CS model.

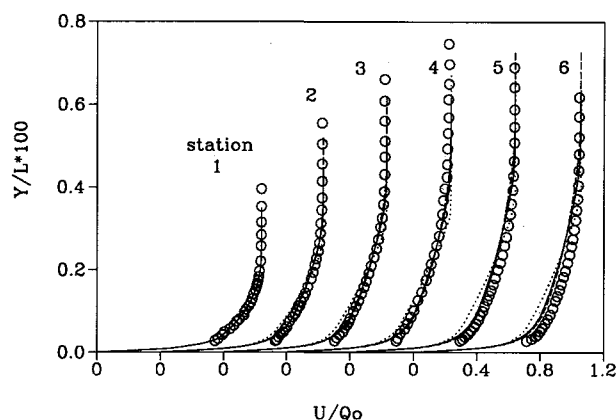


Fig. 10 U -velocity profiles on the windward plane of the combination body, $\alpha = 15$ deg and $Re = 1.86 \times 10^6$: o, experiment; -- present model; - - - ST model; CS model.

6H where ν_t is very much overestimated. This is a direct consequence of the flow divergence, which increases the rate of dissipation and, hence, reduces the eddy viscosity. As is shown in Fig. 8, the vortex stretching invariant χ is negative in most of the region except the small region where the flow is divergent. Accordingly, in the real flow, ν_t increases in most of the outer layer and decreases in the inner region due to the flow convergence and divergence, respectively. Without a proper mechanism to account for this phenomenon, the ST and HL models are unable to compensate for this effect, as the results in Figs. 5-7 show. On the other hand, the present model, which takes account of the influences of the normal stresses as well as the vortex stretching (or squeezing), improves the prediction substantially. Good overall agreement is therefore obtained.

The computational results for the windward plane of symmetry are shown in Figs. 9-12. Along the windward plane of symmetry ($\theta = 0$ deg), the turbulence data are available only in the outer part of the rather thin boundary layer. From the measured pressure distribution shown in Fig. 3, it is seen that the boundary layer on the windward side continuously experiences a mild favorable pressure gradient after a short fetch of adverse pressure gradient upstream of station 1. Because the pressure gradient is fairly small and favorable compared with that in the leeward side, the results of the HL model are nearly identical with those of the ST model. For the sake of brevity, therefore, the results of the HL model are not included here.

Figure 9 shows the variations of the skin friction coefficient and the shape factor along the windward plane of symmetry.

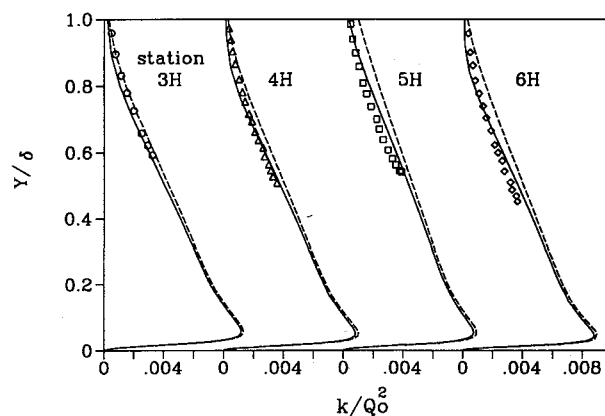


Fig. 11 Turbulent kinetic energy profiles on the windward plane of the combination body, $\alpha = 15$ deg and $Re = 1.86 \times 10^6$: o Δ \square \diamond experiment; -- present model; - - - ST model.

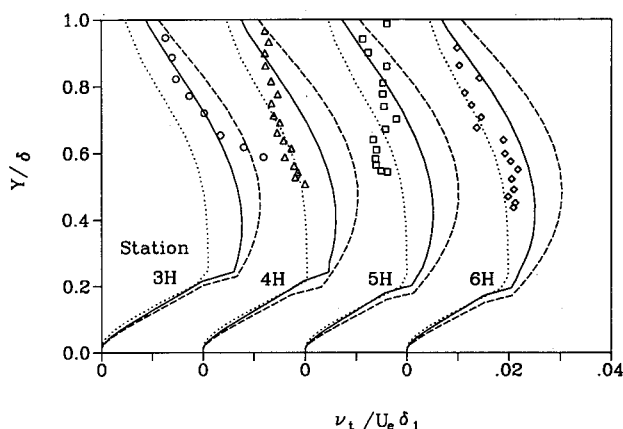


Fig. 12 Eddy-viscosity profiles on the windward plane of the combination body, $\alpha = 15$ deg and $Re = 1.86 \times 10^6$: o, experiment; -- present model; - - - ST model; CS model.

Comparing to the results for the leeward plane of symmetry, both C_f and H are predicted correctly except that the CS model gives higher values of H . The discrepancy in H for the CS model is also revealed in the velocity profiles in Fig. 10: the CS model underestimates the streamwise velocity in the inner half of the boundary layer, whereas the other two models perform satisfactorily throughout the region.

The turbulence quantities k and ν_t are compared in Figs. 11 and 12. The CS model underestimates ν_t early (station 3H) and gradually recovers the correct value at downstream sections. The lower estimate of ν_t is interesting in comparison to the leeward plane-of-symmetry case where ν_t was well overpredicted. The ST model, on the other hand, predicts much larger values of ν_t . This is due to the flow divergence effect that was explained earlier. As can be seen in Fig. 8, the vortex stretching invariant χ is always positive in this plane due to the continuous divergence of the flow, which enhances the dissipation. The correction from the values of the standard k - ϵ model due to the stretching term is substantial, as is seen in Fig. 12. The behavior for the kinetic energy is similar (Fig. 11) although the discrepancy is not so large. The improvement over the ST model is attributed to the lower values of ν_t that, in turn, suppresses the diffusion of the turbulent kinetic energy.

V. Conclusions

In the present study, the role of the vortex stretching and squeezing in the plane-of-symmetry flows is numerically inves-

tigated. Such effects are represented in the formulation of the k - ϵ equations by adding a source term, which is proportional to a vortex stretching invariant in the dissipation rate equation according to the earlier study by Pope.⁴ In addition, the preferential normal stress model of Hanjalic and Launder⁵ is also incorporated. The various flow quantities predicted by the proposed model for a typical plane-of-symmetry flow are compared with those obtained by other models: the standard k - ϵ model, the modified k - ϵ model of Hanjalic and Launder,⁵ which includes the preferential normal stress term, and the mixing length model of Cebeci and Smith.²

Systematic examinations of the predicted profiles, especially those of the turbulent kinetic energy and the eddy viscosity distributions, on the ground of the behavior of W_1 , which represents the flow convergence and divergence, and the vortex stretching invariant χ lead to the following conclusions.

1) Since parameters W_1 and χ vary more widely on the leeward plane of symmetry than on the windward plane, improvements due to the present model is more pronounced in the leeward plane.

2) The preferential normal stress terms correctly represent the effects of the flow convergence (or divergence) and pressure gradient on the variation of k and ν_t .

3) The present numerical study with the proposed model of χ revealed that the stretching of vorticity by the flow divergence suppresses the turbulent kinetic energy k , which, in turn, reduces the turbulent eddy viscosity ν_t , whereas the squeezing plays an opposite role.

4) To simulate correct budget balance of k , both the preferential normal stress and the vortex stretching terms must be incorporated in the model equation. The present comparative study has clearly identified the role of these two terms and demonstrated that the prediction can be markedly improved with this modification.

Acknowledgments

The authors are most grateful to V. C. Patel for reviewing the draft and making many valuable suggestions that improved the paper. Thanks are also due to J. H. Baek for

providing the experimental data and M. U. Kim for his helpful discussions.

References

- ¹Patel, V. C., and Baek, J. H., "Boundary Layer in Planes of Symmetry, Part I: Experiments in Turbulent Flow," *AIAA Journal*, Vol. 25, No. 4, 1987, pp. 550-559.
- ²Cebeci, T., and Smith, A. M. O., "A Finite-Difference Solution of the Incompressible Turbulent Boundary Layers by an Eddy-Viscosity Concept," *Proceedings of the AFOSR-IFP-Stanford Conference: Computation of Turbulent Boundary Layers*, Vol. 1, edited by S. J. Kline, M. V. Morkovin, G. Sovran, and D. J. Cockrell, Stanford Univ, CA 1968.
- ³Patel, V. C., and Baek, J. H., "Boundary Layer in Planes of Symmetry, Part II: Calculations for Laminar and Turbulent Flow," *AIAA Journal*, Vol. 25, No. 6, 1987 pp. 812-818.
- ⁴Pope, S. B., "An Explanation of the Turbulent Round-Jet/Plane-Jet Anomaly," *AIAA Journal*, Vol. 16, No. 3, 1978, pp. 279-281.
- ⁵Hanjalic, K., and Launder, B. E., "Sensitizing the Dissipation Equation to Irrotational Strains," *Journal of Fluids Engineering*, Vol. 102, No. 1, 1980, pp. 34-40.
- ⁶Rodi, W., and Scheuerer, G., "Scrutinizing the k - ϵ Turbulence Model Under Adverse Pressure Gradient Conditions," *Journal of Fluids Engineering*, Vol. 108, No. 2, 1986, pp. 174-179.
- ⁷Nash, J. F., and Patel, V. C., *Three-Dimensional Turbulent Boundary Layers*, SBC Tech Books, Atlanta, GA, 1972.
- ⁸Cutler, A. D., and Johnston, J. P., "The Relaxation of a Turbulent Boundary Layer in an Adverse Pressure Gradient," *Journal of Fluid Mechanics*, Vol. 200, March 1989, pp. 367-387.
- ⁹Chang, K. C., and Patel, V. C., "Calculation of Three-Dimensional Boundary Layer on Ship Forms," Iowa Institute of Hydraulic Research, Univ. of Iowa, Iowa City, IA, IIHR Rept. 178, June 1975.
- ¹⁰Chen, H. C., and Patel, V. C., "Near-Wall Turbulence Models for Complex Flows Including Separation," *AIAA Journal*, Vol. 26, No. 6, 1988, pp. 641-648.
- ¹¹Chen, H. C., and Patel, V. C., "Evaluation of Axisymmetric Wakes from Attached and Separated Flows," *Turbulent Shear Flows 6*, Springer-Verlag, Berlin, 1989, pp. 215-231.
- ¹²Ramaprian, B. R., Patel, V. C., and Choi, D. H., "Mean Flow Measurements in the Three-Dimensional Turbulent Boundary Layer over Bodies of Revolution at Incidence," *Journal of Fluid Mechanics*, Vol. 103, March 1981, pp. 479-504.